Stability of synchronous oscillations in a system of Hodgkin-Huxley neurons with delayed diffusive and pulsed coupling

Enrico Rossoni*
Department of Informatics, Sussex University, Brighton BN1 9QH, United Kingdom

Yonghong Chen and Mingzhou Ding
Department of Biomedical Engineering, University of Florida, Gainesville, Florida 32611, USA

Jianfeng Feng[†]
Department of Mathematics, Hunan Normal University, 410081 Changsha, People's Republic of China
and Department of Computer Science, Warwick University, Coventry CV4 7AL, United Kingdom

We study the synchronization dynamics for a system of two Hodgkin-Huxley (HH) neurons coupled diffusively or through pulselike interactions. By calculating the maximum transverse Lyapunov exponent, we found that, with diffusive coupling, there are three regions in the parameter space, corresponding to qualitatively distinct behaviors of the coupled dynamics. In particular, the two neurons can synchronize in two regions and desynchronize in the third. When excitatory and inhibitory pulse coupling is considered, we found that synchronized dynamics becomes more difficult to achieve in the sense that the parameter regions where the synchronous state is stable are smaller. Numerical simulations of the coupled system are presented to validate these results. The stability of a network of coupled HH neurons is then analyzed and the stability regions in the parameter space are exactly obtained.

I. INTRODUCTION

Synchronous oscillations of neuronal activity have been observed at all levels of the nervous system, from the brainstem to the cortex. The ubiquitous nature of neural oscillations has led to the belief that they may play a key role in information processing. For example, synchronized gamma oscillations have been related to object representation [1], and synchronized neural activity in the somatosensory cortex has been proposed as a mechanism for attentional selection [2].

From a theoretical point of view, the problem of understanding how synchronized oscillations arise has been considered for a variety of systems (see [3] for a review). For neuronal systems, theoretical results are usually obtained under several simplifying assumptions including instantaneous interactions. However, time delays are inherent in neuronal transmissions because of both finite propagation velocities in the conduction of signals along neurites and delays in the synaptic transmission at chemical synapses [4]. It is thus important to understand how synchronization can be achieved when such temporal delays are not negligible [5,6]. Indeed, it has been suggested that time delays can actually *facilitate* synchronization between distant cortical areas.

The study of network models has shown that delayed interactions can lead to interesting and unexpected phenomena [7]. For example, in [8] the authors showed that time delays can induce synchronized periodic oscillations in a network of

diffusively coupled oscillators which exhibited chaotic behavior in the absence of coupling. This was revealed by a stability analysis performed around the synchronized state of the system.

Our goal is to examine whether similar results can be found in biophysical neuronal models, such as the Hodgkin-Huxley (HH) model. Indeed, numerical experiments reported by many authors show that when two systems of the HH type are coupled, they seem to synchronize. Moreover, it has been demonstrated [9] that, in the absence of delay, synchronization takes place for arbitrary initial conditions for a large class of equations including HH models. For delayed interactions, however, an analytical approach to global stability is out of reach, and only local results can be obtained. Here we apply the approach used in [8] to study the stability of the synchronous solutions of coupled HH equations as a function of the coupling strength and time delay. Although the results we obtained are only local, they are still helpful and informative with regards to understanding the mechanisms of synchronization. Moreover, they can be used to reveal regions of the parameter space where two neurons cannot synchronize, regardless of their initial respective conditions.

For two HH neurons coupled diffusively, we found two distinct regions in the parameter space where the synchronized dynamics is stable, and one region where it is not stable. These results, based upon the calculation of the maximum transverse Lyapunov exponent, were then confirmed by numerical simulations.

The results above are found for neurons with diffusive couplings. Pulse coupled neurons, on the other hand, occur far more frequently in the nervous system [10]. Here an approach to tackle the problem of pulse coupling is developed,

---

*Electronic address: e.rossoni@sussex.ac.uk
[†]Electronic address: jianfeng.feng@warwick.ac.uk

which enables us to carry out a general investigation on the stability of synchronized firing of the HH neurons. Our results indicate that whether inhibitory or excitatory interactions can more easily stabilize synchronous firing depends on the quantities we look at. This contrasts with most published results where it is claimed that inhibitory interactions are more effective in inducing synchronization (see, for example [11]).

Finally, we consider networks of HH neurons and determine the parameter regions where synchronous oscillations are found to be stable. Results using similar techniques have appeared in a few other recent publications [12,13], but, to the best of our knowledge, no results on neuronal models have been reported. Although in the current paper we confine ourselves to considering the HH model, our approach can be adopted to investigate more detailed biophysical models of neurons which may, for example, include a wider repertoire of ion channels.

II. MODELS

For a description of the neuronal dynamics we use the Hodgkin-Huxley (HH) model,

$$\dot{V} = \frac{1}{C}[I_{ion}(V,m,h,n) + I_{ext}], \qquad (1)$$

$$\dot{m} = \frac{m_\infty(V) - m}{\tau_m(V)}, \quad \dot{h} = \frac{h_\infty(V) - h}{\tau_h(V)}, \quad \dot{n} = \frac{n_\infty(V) - n}{\tau_n(V)}, \quad (2)$$

where C is the membrane capacitance, V is the membrane potential,

$$I_{ion}(V,m,h,n) = -g_{Na}m^3h(V - V_{Na})dt - g_k n^4(V - V_k)dt$$
$$- g_L(V - V_L)$$

is the total ionic current, and I_{ext} is an externally applied current which we will assume to be constant. For a detailed definition and values of the parameters in the model at a temperature 6.3 °C, we refer the reader to [14,15]. In the following, we will indicate the "gate variables" collectively by the vector $s = (m,h,n)$, and put $C = 1$.

For $I_{ext} < I_1 \approx 6 \ \mu\text{A}/\text{cm}^2$ the system (1) and (2) has a globally attracting fixed point: if excited, the neuron fires a single action potential and then returns to the resting state. Periodic solutions arise at $I_{ext} = I_1$, through a saddle-node bifurcation. For $I_1 < I_{ext} < I_2 \approx 9.8 \ \mu\text{A}/\text{cm}^2$, the system has two attractors, a fixed point and a limit cycle, and the neuron starts showing oscillations of small amplitude around the resting potential. At $I_{ext} = I_2$ the unstable branch of the periodic solutions dies through an inverse Hopf bifurcation, and for $I_{ext} > I_2$ the system has only one attractor which is a limit cycle. In this region, the neuron fires repetitively.

A. Diffusive coupling

We start by considering two identical neurons, represented by the variables V_i, s_i, $i = 1,2$, coupled linearly via their membrane potentials. This type of coupling, usually referred to in the literature as *diffusive* coupling, is appropriate for describing an electrical synapse. For the sake of simplicity, we consider symmetrical coupling. The system is described by

$$\dot{V}_i = I_{ion}(V_i,s_i) + I_{ext} + \epsilon[V_j(t - \tau) - V_i], \quad i,j = 1,2, \quad j \neq i, \qquad (3)$$

where ϵ is the coupling strength, $\tau \geq 0$ is the time delay in the interaction, and the gate variables follow equations similar to Eq. (2).

A *synchronous state* for our system is a solution of Eq. (3) such that

$$(V_1(t),s_1(t)) = (V_2(t),s_2(t)) \qquad (4)$$

for all times t. This state lies on the *synchronization* manifold $(V_1,s_1) = (V_2,s_2)$, which is invariant due to the symmetry of the equations. Given asymmetric initial conditions, we say that the system *synchronizes* if Eq. (4) holds asymptotically. It follows from the definition that, for a synchronous state, we have

$$\dot{V} = I_{ion}(V,s) + I_{ext} + \epsilon[V(t - \tau) - V],$$

$$\dot{s} = \frac{s_\infty(V) - s}{\tau_s(V)}. \qquad (5)$$

In the absence of delay, the equations above reduce to Eqs. (1) and (2), thus, for any value of the bifurcation parameter I_{ext}, each neuron in a synchronous state will behave as if the interaction were absent. In particular, for $I_{ext} > I_2$, the two coupled neurons, once synchronized, will fire periodically as if they were isolated. In the presence of delay, on the other hand, the behavior of a neuron entrained in a synchronous state can be radically different from that of a neuron in isolation. It can be shown that single units displaying a chaotic behavior can be recruited into synchronized periodic oscillations, or periodic oscillators can exhibit synchronized chaos when coupled.

For the synchronous state to be stable, all motions transverse to the synchronization manifold must asymptotically damp out. To examine this, we first reformulate the problem using a more precise notation. By defining $\mathbf{X}^i = (V_i,m_i,h_i,n_i)$ and $\epsilon_1 = (\epsilon_1,0,0,0)$, the system is rewritten as

$$\dot{\mathbf{X}}^i = \mathbf{F}(\mathbf{X}^i) + \epsilon_1 \cdot (\mathbf{X}^j(t-\tau) - \mathbf{X}^i), \quad i,j = 1,2, \quad j \neq i \quad (6)$$

and the synchronous state $\mathbf{X}(t)$ is defined as a solution of

$$\dot{\mathbf{X}} = \mathbf{F}(\mathbf{X}) + \epsilon_1 \cdot (\mathbf{X}(t-\tau) - \mathbf{X}) \qquad (7)$$

where $\mathbf{F}$ is defined by Eq. (5). We now introduce the transverse vector $\mathbf{X}_\perp = \mathbf{X}^2 - \mathbf{X}^1$ and linearize the system (6) around the synchronous state, to obtain

$$\dot{\mathbf{X}}_\perp = \mathbf{J}(\mathbf{X}(t)) \cdot \mathbf{X}_\perp - \epsilon_1 \cdot (\mathbf{X}_\perp(t - \tau) + \mathbf{X}_\perp) \qquad (8)$$

where the matrix $\mathbf{J} = D\mathbf{F}(\cdot)$ is the Jacobian of $\mathbf{F}$. The stability of the synchronous state is now related to the Lyapunov exponents associated with the system (8). Because of the delay term, the system considered is a functional differential equation with an infinite number of Lyapunov exponents. The
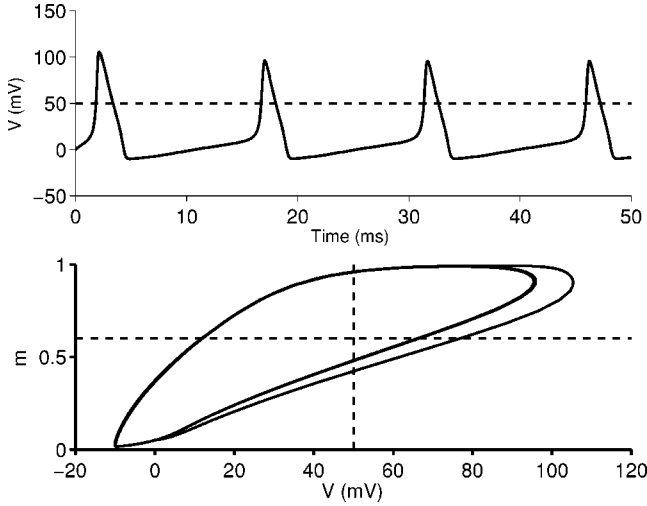
FIG. 1. Solution of Hodgkin-Huxley model for I_{ext} $=10 \ \mu A/cm^2$. (Upper panel) By setting a threshold for the membrane potential ($V = \bar{V} = 50$ mV, dashed line), we cannot distinguish between the upward and downward crossings events. (Lower panel) The two crossing events can be discriminated if an additional threshold for the m-variable is introduced.

synchronous state is stable if all the Lyapunov exponents are negative. This condition is ensured if the *maximum* Lyapunov exponent can be calculated and it is shown to be negative.

B. Pulse coupling

Although numerous examples of electrical synapses have been described in the nervous system of invertebrates and lower vertebrates, the most widespread interaction mechanism among the neurons in the mammalian brain relies on pulselike release of neurotransmitters following action potentials. In order to apply the approach described above to this case, the pulselike interaction must be first put into a convenient mathematical form. In particular, the interaction term must be expressed as a function of the variables of the presynaptic neuron. Hence we consider the following model:

$$\dot{V}_i = I_{ion}(V_i, s_i) + I_{ext} + \epsilon \delta(V_j(t-\tau) - \bar{V}) \Theta(m_j(t-\tau) - \bar{m}),$$

(9)

where $\Theta(\cdot)$ is the Heaviside function, and $\bar{m}$ is a suitably chosen constant. Due to the m-dependent factor in the interaction term, it is possible to select either the upward or the downward threshold crossing event, as it is evident from considering a projection of the spike trajectory on the $V-m$ plane (see Fig. 1). In particular, the interaction term in Eq. (9) will differ from zero only when the membrane potential crosses the threshold from below.

The system is formulated as follows:

$$\dot{\mathbf{X}}^i = \mathbf{F}(\mathbf{X}^i) + \sum_{j=1}^{2} G_{ij} \mathbf{H}(\mathbf{X}^j(t-\tau)), \quad i = 1, 2, \quad (10)$$

where $\mathbf{X}^i = (V_i, s_i), i = 1, 2, \mathbf{G} = [G_{ij}]$ is the coupling matrix given by

$$G_{11} = G_{22} = 0, \quad G_{12} = G_{21} = \epsilon_1, \quad (11)$$

and the interaction term is given by

$$\mathbf{H}(\mathbf{X}) = (H_1, 0, 0, 0) = (\delta(X_1 - \bar{X}_1)\Theta(X_2 - \bar{X}_2), 0, 0, 0).$$

(12)

Linearizing the motion around the synchronous state, we obtain in the transverse direction,

$$\dot{\mathbf{X}} = \mathbf{F}(\mathbf{X}) + \epsilon_1 \cdot \mathbf{H}(\mathbf{X}(t-\tau)), \quad (13)$$

$$\dot{\mathbf{X}}_\perp = \mathbf{J}(\mathbf{X}(t)) \cdot \mathbf{X}_\perp - \epsilon_1 \cdot D\mathbf{H}(\mathbf{X}(t-\tau)) \cdot \mathbf{X}_\perp(t-\tau). \quad (14)$$

Note that, in this case, the synchronous state depends on the coupling even in the absence of delay. Also, because of the nature of the interaction, we have to deal with singular terms in $D\mathbf{H}$. In particular we have

$$\frac{\partial H_1}{\partial X_1} = \delta'(X_1 - \bar{X}_1)\Theta(X_2 - \bar{X}_2) \quad (15)$$

and

$$\frac{\partial H_1}{\partial X_2} = \delta(X_1 - \bar{X}_1)\delta(X_2 - \bar{X}_2), \quad (16)$$

where δ' is the derivative of the delta function in the sense of distributions. Although both terms are highly singular, fortunately a numerical solution of the linearized system is still possible. When a forward Euler scheme is used to solve Eqs. (13) and (14), the two "hard" terms are integrated as

$$A = \int_t^{t+\Delta t} \Theta(m(t'-\tau) - \bar{m})\delta'(V(t'-\tau) - \bar{V})V_\perp(t'-\tau)dt'$$

(17)

and

$$B = \int_t^{t+\Delta t} \delta(m(t'-\tau) - \bar{m})\delta(V(t'-\tau) - \bar{V})m_\perp(t'-\tau)dt'.$$

(18)

Let us consider the term A first. Since the system crosses the m-threshold, $\bar{m}$, and the V-threshold, $\bar{V}$, for different values of t, we have that for all the intervals containing the zeros of the argument of δ', the rest of the integrand is regular. In particular, for all the intervals containing the upward crossing times we will have

$$A = \int_t^{t+\Delta t} \delta'(V(t'-\tau) - \bar{V})V_\perp(t'-\tau)dt'$$

$$= -\frac{\dot{V}_\perp(t_i)}{|\dot{V}(t_i)|} I_{[t+\tau, t+\tau+\Delta]}(t_i)$$

where $\{t_i\}$ indicates the upward crossing times previous of t, and I is the indicator function. On the other hand, during the downward crossing events we will have $A=0$.

As for term B, it is easy to show that, once the "driving" system $\mathbf{X}(t)$ has settled on the attractor, the integrand is al-

ways null, so we can assume $B=0$ for all times during integration.

III. RESULTS

All the differential systems have been integrated numerically using a forward Euler scheme with a time step of 10 μs. A standard technique to calculate the largest Lyapunov exponent, $\lambda_\perp$, consists in averaging the exponential growth rate of the vector $\mathbf{X}_\perp$ along the trajectory [16]. Alternatively, as suggested in [8], the finite time estimate

$$\hat{\lambda}_\perp(T) = \frac{1}{T} \log |\mathbf{X}_\perp(T)| \tag{19}$$

can be used, provided T is a reasonably long time. However, we found this procedure to be prone to errors because of the oscillating behavior of $\log|\mathbf{X}_\perp(t)|$. Instead, a more reliable estimate is obtained by considering the function

$$\xi(t) = \frac{1}{t} \int_0^t \log |\mathbf{X}_\perp(t')| dt'.$$

Indeed, we have asymptotically

$$\xi(t) = \text{const.} + \frac{\lambda_\perp}{2} t + O\left(\frac{1}{t}\right)$$

from where the maximum Lyapunov exponent can be estimated.

A. Diffusive coupling

For the case of diffusive coupling, we have considered a range of values for the applied current stimulus I_{ext}=7, 10, 15, and 20 μA/cm^2. For all these values, the isolated neurons fire periodically. Simulation results show that $\lambda_\perp$ is always negative on the semiaxis ($\tau=0, \epsilon>0$), regardless of the amplitude of the current stimulus considered (see Fig. 2). Therefore two identical HH neurons with symmetrical coupling will always synchronize in the absence of delays, no matter how small the coupling is. This result is consistent with what was shown in [9]. As expected, $|\lambda_\perp|$ increases monotonically with ϵ, indicating that the system synchronizes more rapidly with stronger coupling.

The (ϵ, τ) space is characterized by a predominance of stable solutions. However, the plot of Fig. 2 reveals three distinct regions (left panel, Fig. 2), which correspond to different behaviors of the solutions of the coupled system (3). Direct simulations revealed that in the region at the bottom of each graph, the synchronous state is represented by ordinary oscillations, and that this state is globally attractive. Therefore, in this region, two neurons will eventually synchronize, regardless of their initial phase. However, the synchronous state, and its stability, change with τ. In particular, when τ is increased above the first boundary line, the amplitude of the limit cycle on the synchronous manifold is suddenly reduced, and we observe the phenomenon of oscillation death (see Fig. 3 upper left). In order to display this behavior, the neuron must still have a stable resting state, albeit with a small basin of attraction. Therefore oscillation

death will only be observed in the region of bistability $I_1 < I_{ext} < I_2$. Note that, because of the term $-\epsilon V(t)$, the region of bistability of the model with self-interaction is different from that of the isolated model, thus explaining why the quenched oscillations can be observed also in the other cases considered here. In the region between the two boundary lines, this state is locally attractive for the dynamics of the complete system, thus we see coupled neurons reciprocally suppressing their oscillations. Occasionally, depending on the initial conditions and the choice of the parameters, we observed the coupled system desynchronizing and settling in an antiphase locked oscillatory state (see Fig. 3 upper right). The "hot-spot" near the upper left corner of Fig. 2 is indicative of a different attractor on the synchronous manifold, which looks like that shown in Fig. 3 (bottom left). In this case, the time delay is such that the current pulse, due to the self-interaction, is delivered too late to switch the system to the resting state, yet too early to anticipate the onset of the next spike. However, we found that these oscillations are very easily destabilized, and the complete system is attracted to the antiphase locked state. Finally, in the region above the upper boundary line, the synchronous state is again oscillatory, although the firing rate is now almost twice as much as that of the isolated neurons. This is due to the self-interaction pulse which follows each spike, which now is delivered sufficiently late, and with a sufficient amplitude, to overcome refractoriness and anticipate the occurrence of the following spike (see Fig. 3 bottom right).

In Fig. 4 we depicted the period of the oscillations, T, observed by simulating the coupled system. The figure has to be viewed together with Fig. 2. Below the unstable region, the values reported correspond to the period of the synchronous oscillations. In the region (middle) where the synchronous state is not stable, the observed period is that of antiphase locked solutions. The points where $T=0$ (that appear as dark blue "holes" in the graph) mark the values of the parameters for which quenched oscillations were observed. In the upper region, a mixed phenomenon is observable, with the seemingly random occurrence of synchronized and antiphase locked states. This plot shows clearly the sudden drop of the period across the lower boundary line, which marks the onset of an attractive antiphase locked oscillatory state in the entire system's phase space. The predominance of solutions with $T \neq 0$ demonstrates that although quenched oscillations (the "holes" at $T=0$) are locally stable in this region, the antiphase locked state has a much larger basin of attraction. For longer delays, we observe instead a mixture of two phases corresponding to synchronous and antiphase locked oscillations, which indicates that the actual synchronization, for these values of the coupling parameters, is largely dependent on the initial conditions of the system.

In summary we presented a systematic study for two diffusively coupled HH neurons, in terms of the Lyapunov exponent and confirmed by direct simulations. It is generally easy to synchronize two neurons due to the nature of interactions. We also presented a MATLAB program (http://www.informatics.sussex.ac.uk/users/er28/synchronization/) to demonstrate the results presented here.
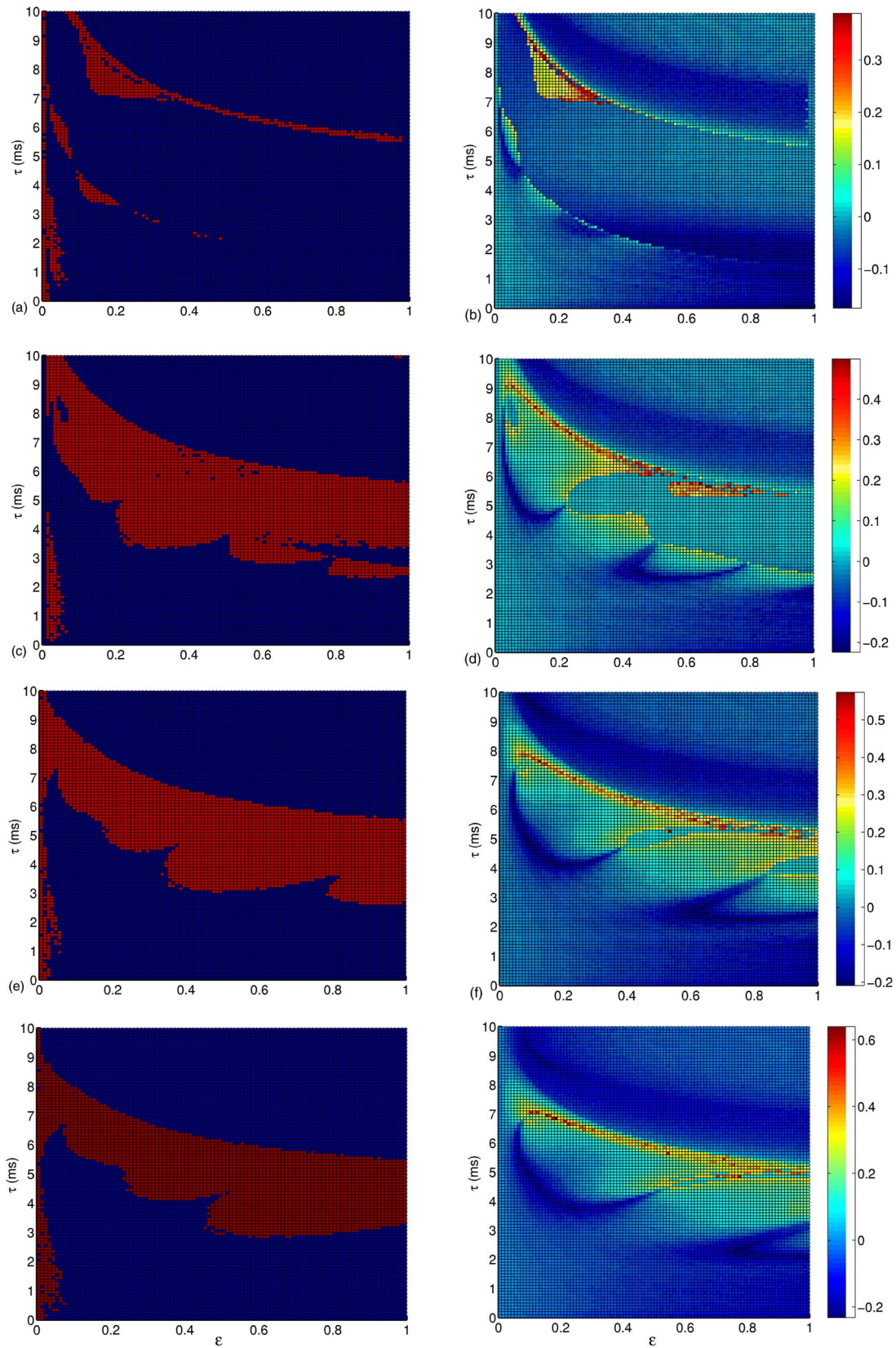
FIG. 2. (Color online) Stability of synchronized oscillations for a system of two HH neurons with diffusive coupling. (Right) Color intensity represents the maximum transverse Lyapunov exponent, $\lambda_\perp$, in the $(\tau-\epsilon)$ space. (Left) Similar to the right figures, but it represents the region of stability (blue) and unstable regions (red) in the $(\tau-\epsilon)$ space. Results were obtained for $I_{ext}=7$, 10, 15, and 20 $\mu A/cm^2$ (from top to bottom).
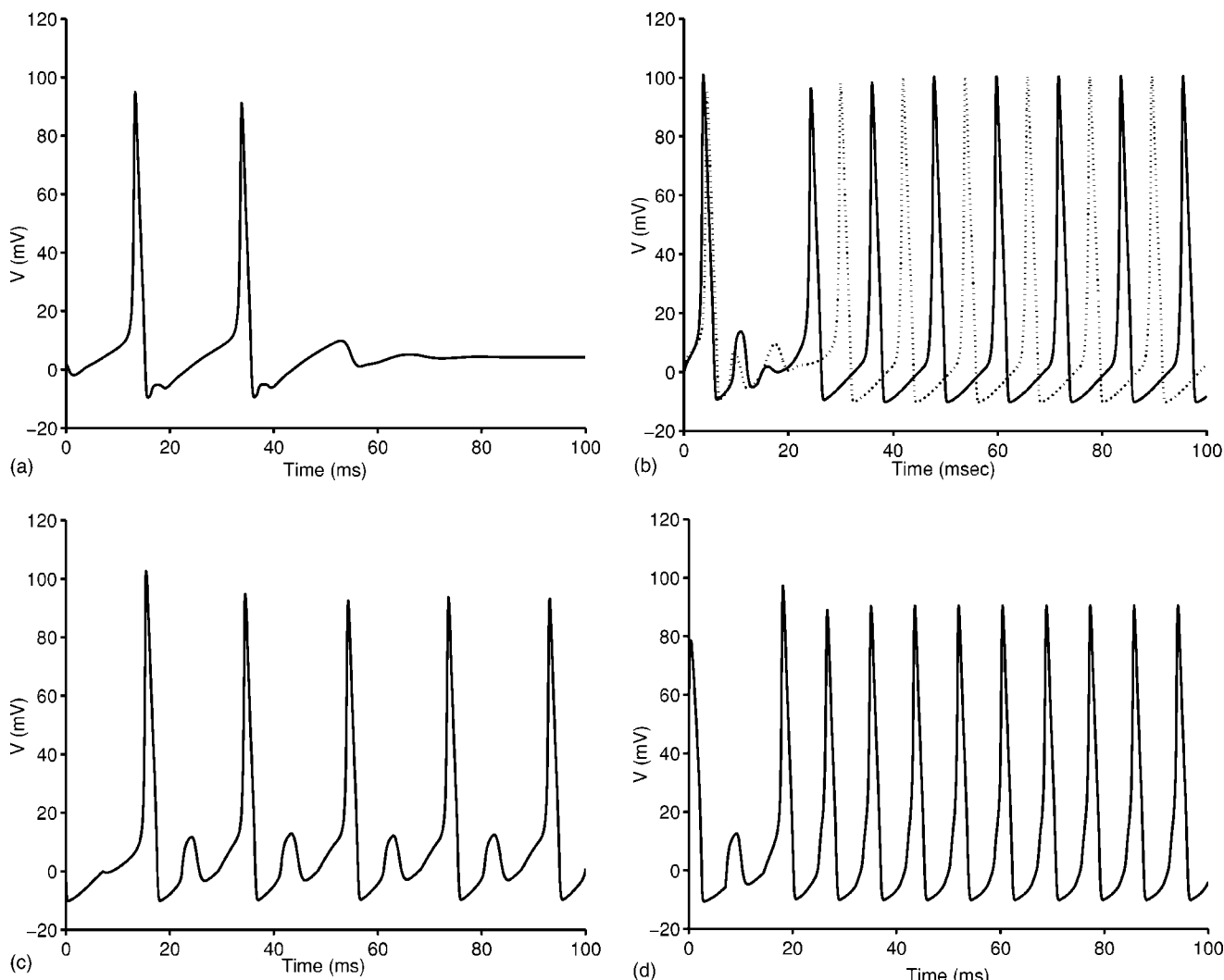
FIG. 3. $I_{ext}=7$ μA/cm^2. Upper left: The phenomenon of "oscillation death" for an HH neuron with delayed self-interaction ($\epsilon=0.22$, $\tau=3.3$ ms). Upper right: Antiphase locking for two HH neurons with delayed interaction ($\epsilon=0.58$, $\tau=5.33$ ms). Bottom left: Oscillatory behavior in the synchronous state is recovered after increasing time delay ($\epsilon=0.15$, $\tau=7.1$ ms). Bottom right: Self-interaction can anticipate firing if coupling is large enough to overcome refractoriness ($\epsilon=0.5$, $\tau=7.1$ ms).

B. Pulse coupling

Figure 5(a), shows the maximum transverse Lyapunov exponent of the system (13) and (14), as a function of (ϵ, τ). Here we considered also negative values of ϵ to represent a reciprocal inhibitory coupling.

Figure 5(b) and (c), also shows two "sections" at $\epsilon=-4$ and 4 mV. In order to validate these results, we considered the behavior of the solutions of the system (13) and (14) for different values of (ϵ, τ). First, we set arbitrary initial conditions on the synchronous manifold, $\mathbf{X_1}=\mathbf{X_2}$, and let the system settle onto the attractor. After a transient, the system is displaced out of the synchronous manifold by an instantaneous perturbation on V_1, $V_1 \rightarrow V_1 + \delta V$, and then it is left to evolve unperturbed. In Fig. 6 we reported some of the calculated trajectories projected onto the (V_1, V_2) plane. These plots illustrate the qualitatively distinct behaviors that are observed for different values of ϵ and τ, including synchronization, phase locking, antiphase locking, and possible

chaos. For all the cases considered, the observed behavior was found to be consistent with the calculated Lyapunov exponent.

We observed that, when the synchronous state is stable, the type of attractor that lies outside its basin of stability depends on the sign of the coupling. In particular, if the coupling is positive, the solution is attracted onto a phase-locked state (Fig. 6 upper right), whereas for negative coupling a chaotic attractor seems to be present (see Fig. 6 bottom right). Also we noticed that the two branches around the minimum in Fig. 6 (bottom left) correspond to a change in the structure of the attractors around the synchronous manifold. In particular, for the left branch the synchronous state is very stable, as if it was the only attractor in the whole space, while for the right branch the stability of the synchronous state is lost by being attracted onto a seemingly chaotic state.

Finally, we can now address the issue of whether inhibitory or excitatory interactions can facilitate synchronization. In the literature, it is often reported that inhibitory, but not
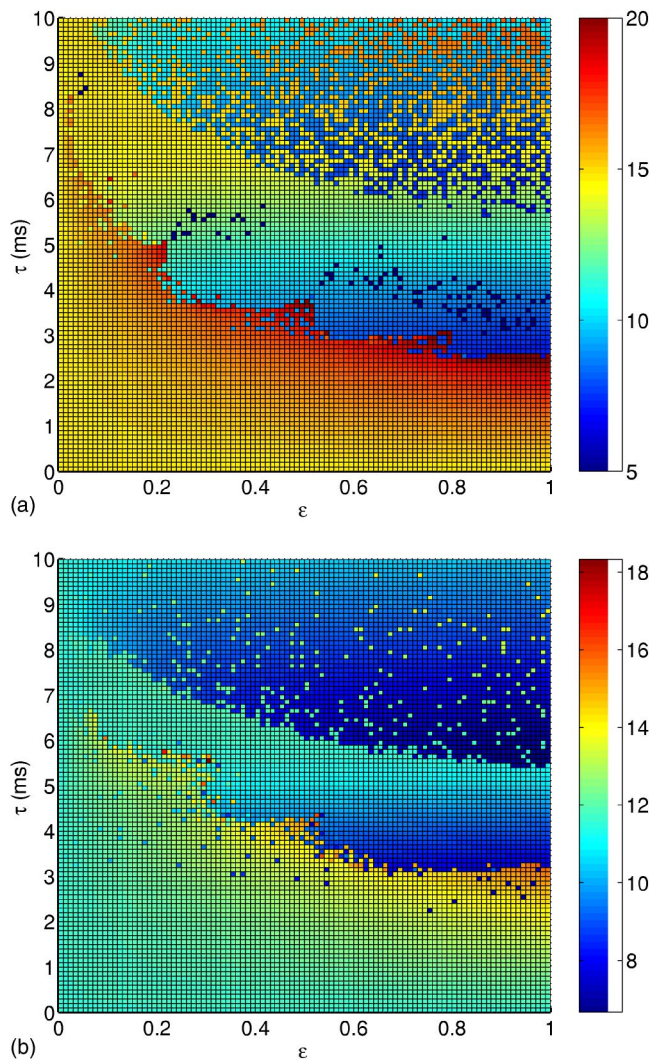
FIG. 4. (Color online) The period T of the oscillations as observed in a system of two diffusively coupled HH neurons. Results were obtained for $I_{ext}=10$ μA/cm^2 (top) and $I_{ext}=20$ μA/cm^2 (bottom). For fixed parameters, the initial state is chosen randomly and the quenched state (middle region) is represented by a "hole" in the figure, comparing with Fig. 2.

excitatory interactions, can synchronize two neurons, a result that is based upon analysis of the leaky integrate and fire model. Our results tell us that, for the HH model, *both* excitatory and inhibitory interactions can synchronize neuronal activity. Figure 7(a), does show that in terms of the magnitude of the Lyapunov exponent, inhibitory interactions have a more negative value and so it is more stable in this sense, in agreement with results in the literature. However, when we look at the sign of the Lyapunov exponent, we have a totally different scenario. With excitatory interactions the regions in which the Lyapunov exponent are negative are bigger than that with inhibitory interactions [Fig. 7(b)]. In fact, the averaged sign (λ) is always positive when the interaction is negative.

C. Synchronization in time-delayed networks

Now we consider a system containing an arbitrary number of neurons with general coupling topologies. This can be
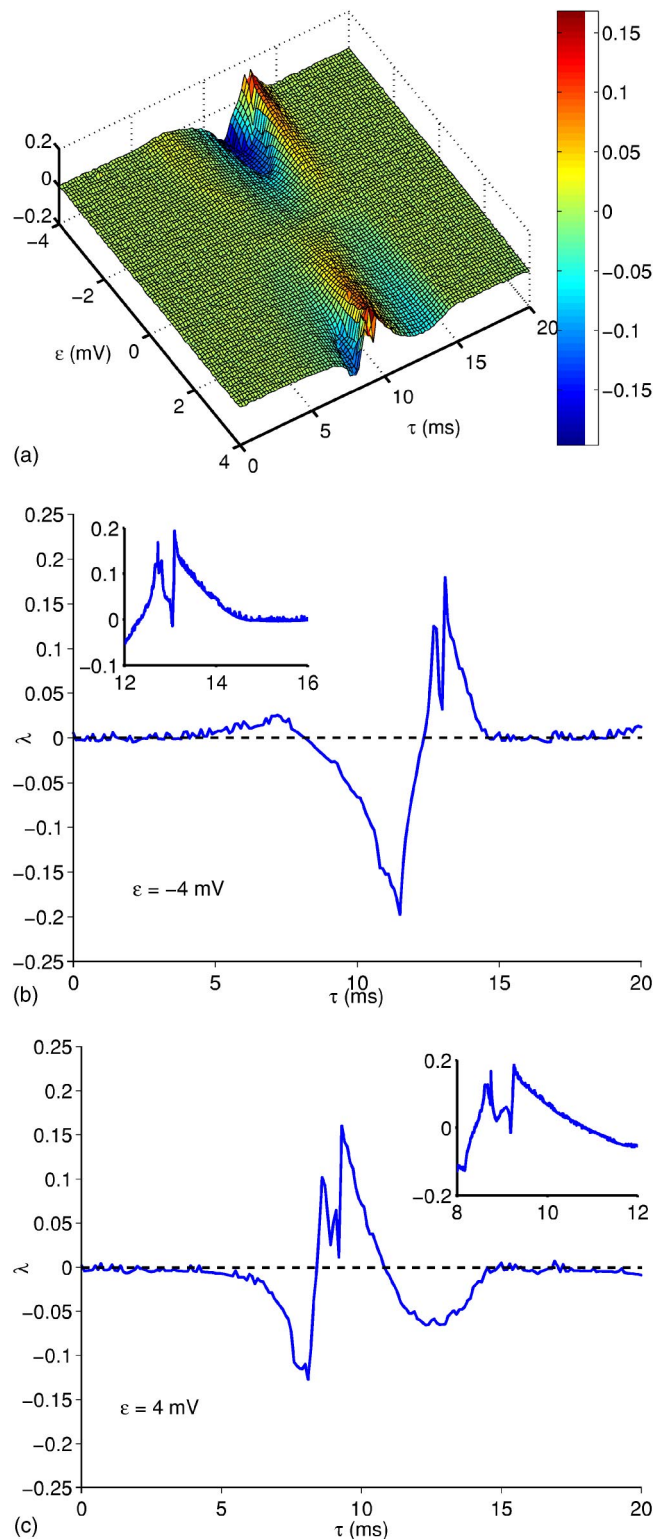

FIG. 5. (Color online) (a) Stability of synchronized oscillations for a system of two HH neurons with pulse coupling. Color intensity represents the maximum transverse Lyapunov exponent, $\lambda_\perp$, in the $(\tau-\epsilon)$ space. Results were obtained for $I_{ext}=10$ μA/cm^2. (b) The maximum transverse Lyapunov exponent, $\lambda_\perp$, as a function of time delay for $\epsilon=-4$ mV. The inset shows a blowup around the maximum. (c) The maximum transverse Lyapunov exponent, $\lambda_\perp$, as a function of time delay for $\epsilon=4$ mV.
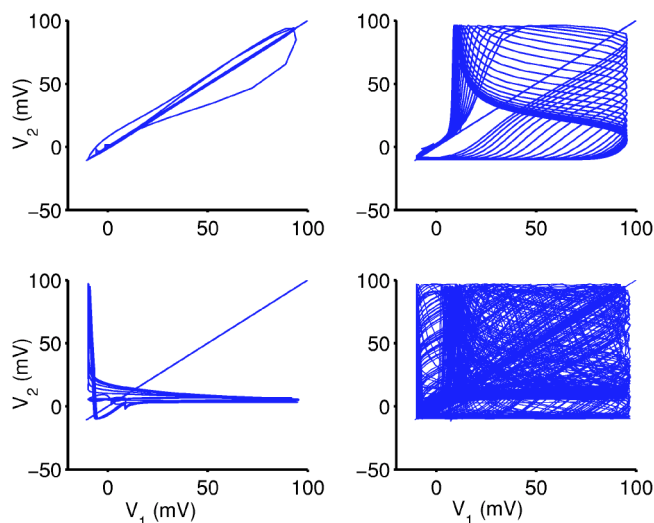
FIG. 6. Examples of trajectories in the V_1-V_2 plane which correspond to different dynamical behaviors: synchronization (top left; $\epsilon=3$ mV, $\tau=8$ ms); antiphase locking (bottom left, $\epsilon=4$ mV, $\tau=13$ ms); phase-locking (top right, $\epsilon=-2$ mV, $\tau=8$ ms); and chaos (bottom right $\epsilon=-4$ mV, $\tau=11.6$ ms). The system is initialized on the synchronous manifold and left to evolve freely until an instantaneous perturbation is applied which disrupts the symmetry of the solution. The trajectories in the V_1-V_2 reveal different kinds of attractors, which are manifest when the synchronous manifold is destabilized. For positive coupling (upper panels), once displaced out of the synchronous manifold, the system gets attracted to a phase-locked oscillatory state; for negative coupling (lower panels), the system shows aperiodic oscillations which are indicative of a seemingly chaotic (strange) attractor.

done following the scheme used by Pecora and Carroll [17]. Given a system of N interacting HH neurons, with coupling matrix **G**,

$$\dot{\mathbf{X}}^i = \mathbf{F}(\mathbf{X}^i) + \sum_j G_{ij}\mathbf{H}(\mathbf{X}^j(t-\tau)) \qquad (20)$$

the stability problem, originally formulated in a $4 \times N$ dimensional space, can be reduced to the study of the system

$$\dot{\xi}(t) = \mathbf{J}(\mathbf{X}(t))\xi(t) + (\alpha+i\beta)D\mathbf{H}(\mathbf{X}(t-\tau))\xi(t-\tau), \quad (21)$$

where $\alpha+i\beta$ is an eigenvalue of **G**, in general complex-valued, and ξ is a four-dimensional perturbation vector. To ensure that the synchronized state $\mathbf{X}^i=\mathbf{X}$ is a solution of the dynamics, we require that

$$\sum_j G_{ij} = 0, \quad i=1,\ldots,N. \qquad (22)$$

By separating ξ into the real part ξ_r and imaginary part ξ_i, we get

$$\dot{\xi}_r = \mathbf{J}(\mathbf{X})\xi_r + \alpha D\mathbf{H}(\mathbf{X}_\tau)\xi_{r\tau} - \beta D\mathbf{H}(\mathbf{X}_\tau)\xi_{i\tau}, \qquad (23)$$

$$\dot{\xi}_i = \mathbf{J}(\mathbf{X})\xi_i + \alpha D\mathbf{H}(\mathbf{X}_\tau)\xi_{i\tau} + \beta D\mathbf{H}(\mathbf{X}_\tau)\xi_{r\tau}, \qquad (24)$$

where $\xi_{r\tau}=\xi_r(t-\tau)$ and $\xi_{i\tau}=\xi_i(t-\tau)$. For a given value of τ, we can consider α, β as parameters and estimate the maxi-
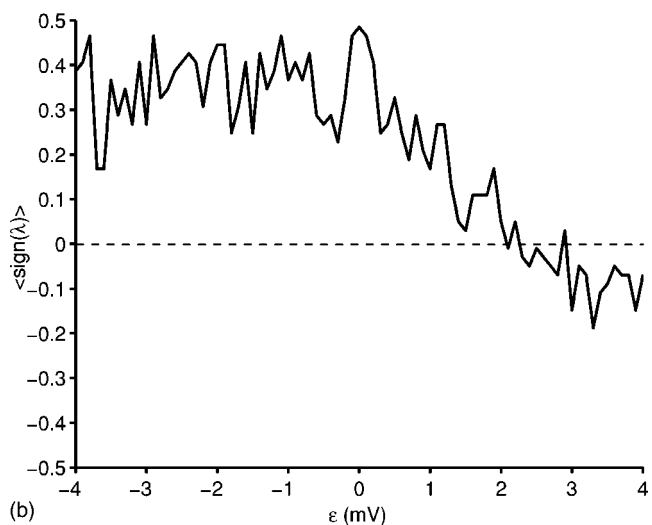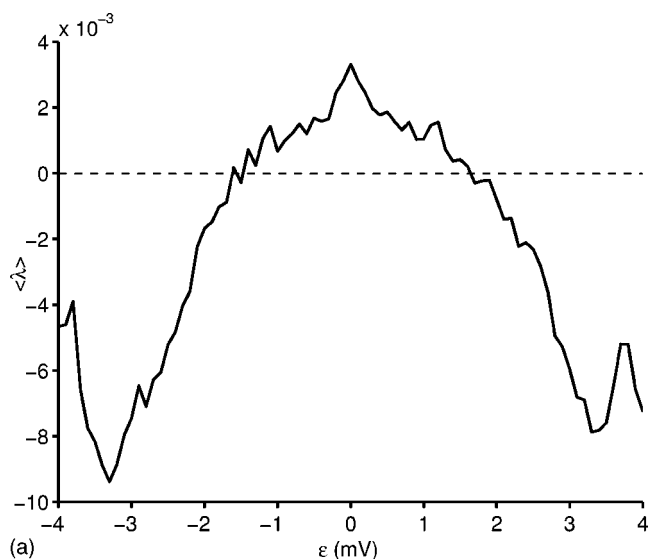

FIG. 7. (a) Average of $\lambda_\perp$ over $\tau \in [0,20]$ ms; and (b) average of $\text{sign}(\lambda_\perp)$ over $\tau \in [0,20]$ ms.

mum Lyapunov exponent $\lambda_{\perp,max}$ from Eqs. (23) and (24). This function is known as the master stability function and defines a region of stability of the synchronous oscillations in terms of the eigenvalues of the coupling matrix. Given a particular network topology and a value of the time delay, the synchronous state will be stable if, and only if, all the eigenvalues of the coupling matrix lie in the region of stability indicated by the master stability function.

The plots of Fig. 8 show the results obtained for the diffusive coupling case, for an external stimulus of $I_{ext}=10$ μA/cm^2 and different values of the delay. The stability region becomes smaller as the delay increases. It is interesting to compare the results in the current section with that in Sec. III A. It is easily seen that we have two eigenvalues for two HH models with diffusive coupling: one is $\alpha=-2\epsilon, \beta=0$ and the other is $\alpha=0, \beta=0$. To apply the results in the previous section to the case in this section, we see that the second eigenvalue lies on the boundary of the stable and unstable region. Nevertheless, a more detailed analysis tells us that in fact the results cannot be applied to the cases
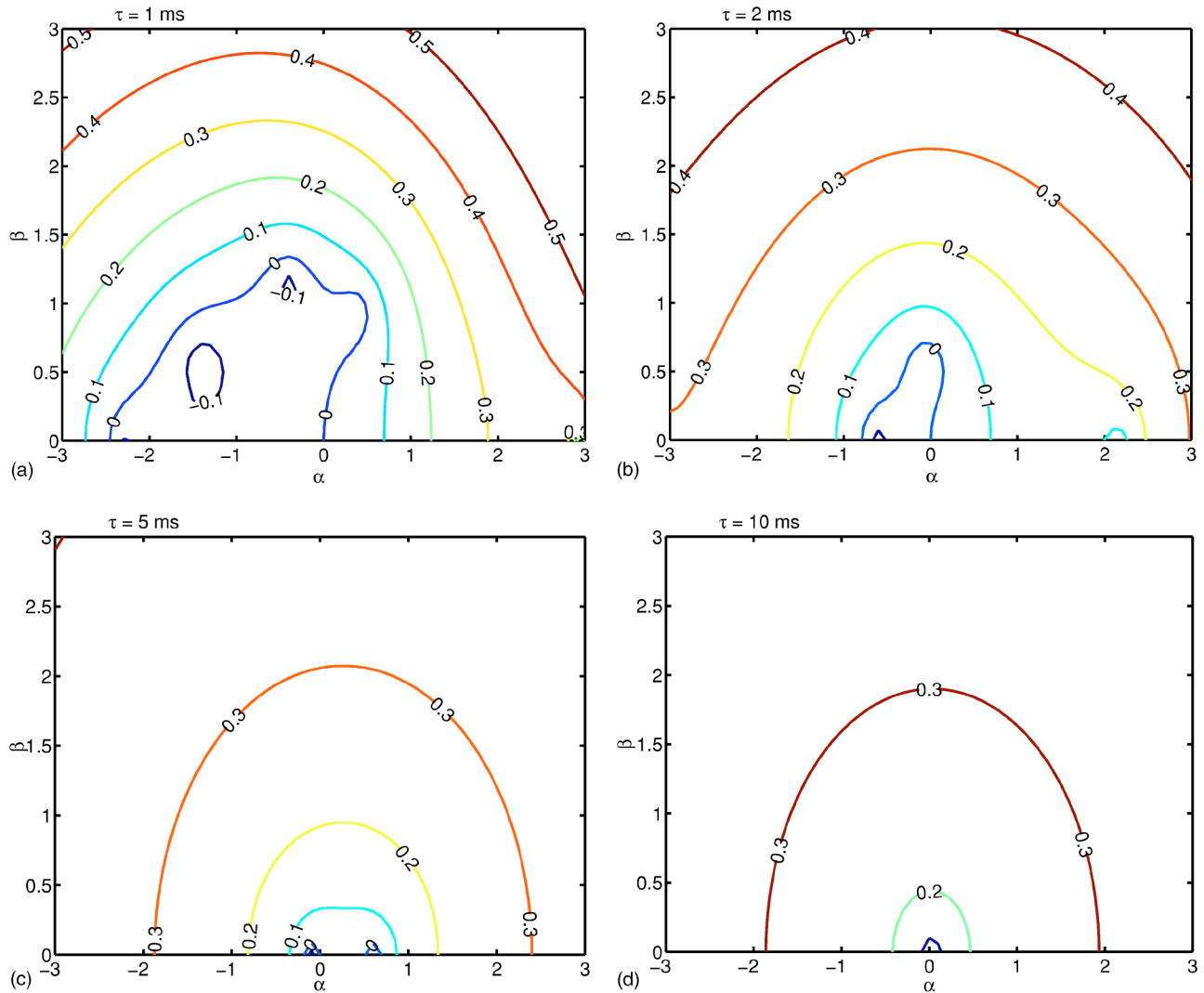
FIG. 8. (Color online) Upper panel: Master stability function at $\tau=1$ ms (a) and $\tau=2$ ms (b), for a system of diffusively coupled HH neurons. The lines are isoclines for the constant maximum Lyapunov exponent. Bottom panel: Master stability function at $\tau=5$ ms (c) and $\tau=10$ ms (d), for a system of diffusively coupled HH neurons. The lines are isoclines for the constant maximum Lyapunov exponent.

considered in Sec. III A. The interaction term in Sec. III A does not vanish, but it is zero due to the constraint (22) for the system (20). Of course, the results presented in Fig. 8 are general enough for an arbitrary interaction matrix satisfying the constraint (22).

In Fig. 9 we depicted the results for the pulse coupling case, obtained for the same values of I_{ext} and τ as for the diffusive coupling case above. Again it is worth noting that the dynamics considered here actually differ from that considered in the previous section, since we require that $\Sigma_j G_{ij} = 0$. Since real neurons are either excitatory or inhibitory, we have that, for fixed j, G_{ij} must have the same sign, either positive or negative, for all i. However, for a system of two neurons, it is impossible to implement such a coupling scheme if we exclude self-interaction, so the results presented here are totally different from what we discussed in the previous section, as in the case of diffusive coupling. It is very interesting to observe that the constraint (22) requires that the total excitatory and inhibitory inputs to each neuron be balanced, a condition which is extensively discussed in

the literature. We also note that the stability region for the synchronization state gets smaller with increasing delay τ.

IV. DISCUSSION

We presented a systematic study of the synchronization properties of groups of neurons coupled with diffusive or pulse delayed interactions. In particular, for two HH neurons coupled diffusively, we found that there are three distinctive regions where different behaviors are observable. For two HH neurons with pulse coupling, it is found that excitatory coupling tends to synchronize more easily their activity. Not surprisingly, gap junction, rather than pulse coupling, has a wider parameter region where neuronal activity can be synchronized. That could be easily understood from the general dynamics: electrical coupling tends to minimize both subthreshold and suprathreshold dynamics, while pulse coupling acts only when a spike is fired (suprathreshold). Finally, a few general results on the stability of synchronized oscillations in networks of HH neurons are presented.
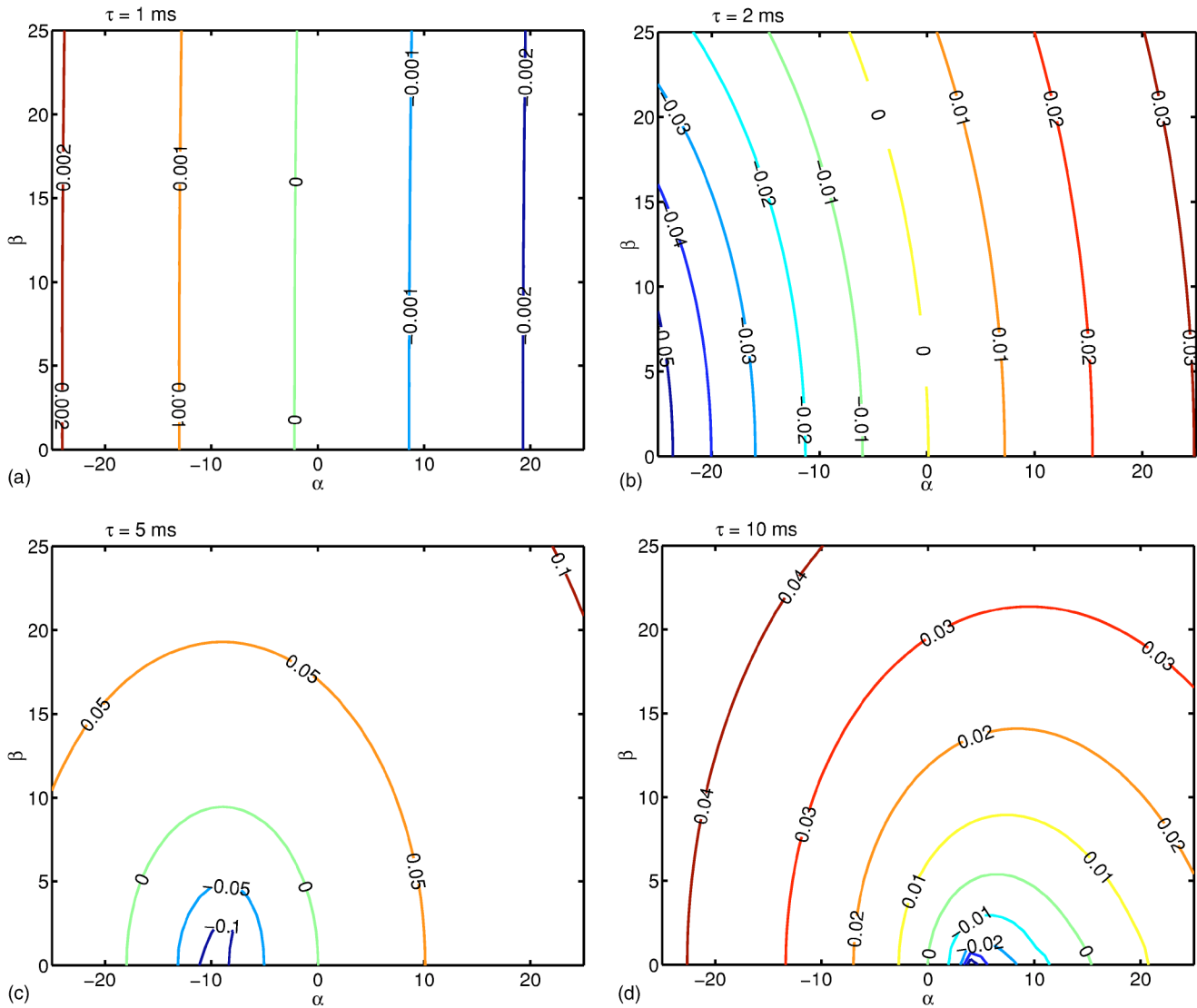
FIG. 9. (Color online) Master stability function at $\tau=1$ ms (a), $\tau=2$ ms (b), $\tau=5$ ms (c), and $\tau=10$ ms (d), for a system of pulse coupled HH neurons. The lines are isoclines for the constant maximum Lyapunov exponent.

Theoretical studies such as the one we presented here have a number of limitations. For example, we have to require that the neurons be identical in order to perform our analysis, which is obviously an oversimplification of real neuronal networks. For a network of nonhomogeneous neurons, it is more realistic to consider phase synchronizations. Also, we do not expect that exact synchronization holds in the presence of noise, and jitters in real neurons may totally change the results presented here. One can also argue that desynchronization rather than synchronization might be more important for information processing in the nervous system.

In spite of these limitations, our results are interesting in several respects. For example, if we can figure out the exact regions where a system of neurons will synchronize, then outside these regions the system will desynchronize. Besides, the current results concerning the dynamics of networks of neurons, combined with the approach we presented in [12], can be easily extended to analyze networks of neuronal models with random interactions such as in microcolumn networks [18,19].

[1] W. Singer *et al.*, Trends in Cognitive Science **1**, 252 (1997).

[2] P. N. Steinmetz *et al.*, Nature (London) **404**, 187 (2000).

[3] A. Pikovsky, M. Rosenblum, and J. Kurths, *Synchronization—A Universal Concept in Nonlinear Science* (Cambridge University Press, Cambridge, England, 2001).

[4] E. R. Kandel, J. H. Shwartz, and T. M. Jessel, *Principles of Neural Science* (Elsevier, New York, 1991).

[5] A. K. Engel, P. Konig, A. K. Kreiter, and W. Singer, Science **252**, 1177 (1991).

[6] R. Ritz and T. J. Sejnowski, Curr. Opin. Neurobiol. **7**, 536 (1997); W. Singer and C. M. Gray, Annu. Rev. Neurosci. **18**, 555 (1995); U. Ernst, K. Pawelzik, and T. Geisel, Phys. Rev. Lett. **74**, 1570 (1995); W. Gerstner, *ibid.* **76**, 1755 (1996); I. S. Labouriau and C. Alves-Pinto, Bull. Math. Biol. **66**, 539 (2004); V. K. Jirsa and M. Ding, Phys. Rev. Lett. **93**, 070602 (2004); J. M. Casado and J. P. Baltanas, Phys. Rev. E **68**, 061917 (2003); T. Bem and J. Rinzel, J. Neurophysiol. **91**, 693 (2004).

[7] F. M. Atay, J. Jost, and A. Wende, Phys. Rev. Lett. **92**, 144101 (2004).

[8] M. Dhamala, V. K. Jirsa, and M. Ding, Phys. Rev. Lett. **92**, 074104 (2004).

[9] I. S. Labouriau and H. M. Rodrigues, Dynam. Cont. Dis. Ser. A 10, 463 (2003).

[10] J. F. Feng, *Computational Neuroscience: A Comprehensive Approach* (Chapman and Hall/CRC Press, Boca Raton, 2003).

[11] C. van Vreeswijk, L. F. Abbott, and G. B. Ermentrout, J. Comput. Neurosci. **4**, 313 (1994).

[12] Y. Deng, M. Ding, and J. F. Feng, J. Phys. A **37**, 2163 (2004).

[13] J. G. Restrepo, E. Ott, and B. R. Hunt, Phys. Rev. Lett. **93**, 114101 (2004).

[14] D. Brown, J. F. Feng, and S. Feerick, Phys. Rev. Lett. **82**, 4731 (1999).

[15] A. Hodgkin and A. Huxley, J. Physiol. (London) **117**, 500 (1952).

[16] J. P. Eckmann and D. Ruelle, Rev. Mod. Phys. **57**, 617 (1985).

[17] L. M. Pecora and T. L. Carroll, Phys. Rev. Lett. **80**, 2109 (1998).

[18] W. Maass, T. Natschlger, and H. Markram, in *Computational Neuroscience: A Comprehensive Approach*, edited by J. F. Feng (Chapman and Hall/CRC Press, Boca Raton, 2003), Chap. 18, pp. 575–605.

[19] A. Destexhe and E. Marder, Nature (London) **431**, 789 (2004).